A Lane-group Based Macroscopic Model for Signalized Intersections Account for Shared Lanes and Blockages

Yue Liu, Gang-Len Chang, Jie Yu, Yuanyuan Hou, and Saed Rahwanji

***Abstract* — This paper presents a macroscopic model of traffic able to replicate the key features occurring at signalized intersections. Different from the previous link or movement based traffic flow models, the proposed model considers explicitly queue accumulation and dissipation at the lane-group level, in order to facilitate modeling the discharging process for shared lanes. In particular, the proposed model also accounts for the blocking effects between different lane groups due to intersection geometric constraints or improper signal settings, which offer potentials for it to be integrated with optimal control models. The performance of the proposed model applied to a real-world intersection under different demand levels appears to be computer-efficient and convincing when validated by a calibrated microscopic simulation program, VISSIM.**

I. INTRODUCTION

THE vehicular delay at signalized intersections, which increases the travel time as well as reduces speed and reliability, is an obstacle that has a detrimental effect on cost-effectiveness of transportation system. Therefore, it has been the traffic engineer's endeavor to model the operation of dynamic traffic systems and helps analyze the causes and potential solutions of traffic problems such as congestion and safety. Various traffic flow models and simulation techniques have evolved and aided traffic engineer in this process. The level of detail in those models ranges from microscopic via meso-scopic to macroscopic. Microscopic and meso-scopic simulation models, integrated into well known programs such as CORSIM, VISSIM, PARAMICS, SIMTRAFFIC, and TRANSMODELER, can emulate traffic at signalized intersections in details. However, concerns are often expressed regarding their complexity to calibrate lots of behavioral parameters and its stochastic nature which requires several runs for obtaining representative results. Therefore, their potentials to be incorporated into the optimal control models are restricted. On the contrary, macroscopic approaches have much fewer parameters which can be easily calibrated, and require much less burden of computation time and computer storage which make them well suitable to be integrated into optimal control models or large-scale applications.

A variety of approaches have been proposed in the literature to describe traffic flows in urban arterials in a macroscopic way. Kashani et al. [1] have developed an urban arterial traffic flow model based on horizontal queues and large time steps. The cell transmission models [2][3] were also proposed and revised to model urban traffic flows. Wu and Chang [4] formulated a series of dynamic traffic state evolution equations with a flow transition mechanism between adjacent roadway segments and links. Two-phase signals were modeled with G/C ratios instead of green splits, offsets, and cycle lengths. Van den Berg et al. [5] proposed a modified and extended version of Kashani's model which is able to capture individual movement-based horizontal queues and take into account the blocking effect due to the downstream spillback. Many existing traffic signal optimization programs, such as SYNCHRO and TRANSYT-7F [6] have developed their own deterministic macroscopic models. Despite the promising work by the previous studies, the following drawbacks remain to be further addressed:

- Previous studies model the dynamic queue evolution either at a link-based level or at an individual movement-based level, which could result in either difficult integration with multiple signal phases or inaccurate modeling of queue discharging rates when there are shared lanes in the target intersection approach;
- Vehicle arrival process in many studies was modeled by assumption of free-flow speeds from the link upstream to the end of the queue, which is inappropriate under congested traffic conditions;
- The blocking effects between different movements or lane groups are neglected. For example, the left turn traffic with insufficient left turn pocket capacity could block the through traffic.

To accommodate the aforementioned issues as well as to ensure the computational efficiency, this study proposes a set of lane-group-based formulations.

II. MODEL FORMULATION

This section proposes a set of enhanced dynamic equations for detailed modeling of signalized intersections using the

Manuscript received June 1st, 2008.

Y. Liu is Research Assistant at University of Maryland at College Park, College Park, MD 20742 USA (e-mail: troybest@ umd.edu).

G.L. Chang is Professor at University of Maryland at College Park, College Park, MD 20742 USA (e-mail: gang@umd.edu).

J. Yu is Research Associate at University of Maryland at College Park, College Park, MD 20742 USA (e-mail: yujie@umd.edu).

Y. Hou is Research Assistant at University of Maryland at College Park, College Park, MD 20742 USA (e-mail: cnhyyde@umd.edu).

S. Rahwanji is the Traffic Engineering Team Leader at Maryland State Highway Administration, 7491 Connelley Drive, Hanover, MD 21076 USA (e-mail: SRahwanji@sha.state.md.us).

concept of lane-group based queue. The potential model should have the ability to address the following requirements:

- It should satisfy both computational efficiency and modeling accuracy;
- It should capture the dynamic evolution of physical queues with respect to the signal status, arrivals, departures, and blocking effects;
- It should be able to model the merging and splitting of vehicle movements at intersections;
- It should be able to handle both light and congested traffic conditions;

A. *Model Parameters and Variables*

To facilitate the presentation of model formulations, this section summarizes the notations of major parameters and variables used in the model:

Δt: update interval of system status,

T: The time horizon under consideration (in #. of Δt),

k: Time step index corresponds to time $t = k\Delta t$,

S^U: Set of links,

S_r: Set of demand origins,

P: Set of signal phases at the intersection,

$p, p \in P$: Index of signal phase at the intersection,

$i, i \in S^U$: Index of links,

$\Gamma(i)$: Set of upstream links of link i,

$\Gamma^{-1}(i)$: Set of downstream links of link i,

l_i: Length of link i,

n_i: Num. of lanes in link i,

N_i: Storage capacity of link i,

Q_i: Discharge capacity of link i,

ρ^{jam}: Jam density,

v_i^{free}: Free flow speed at link i,

$v^{\min}$: Minimum speed corresponding to the jam density,

α, β: Constant model parameters,

S_i^M: Set of lane groups at link i,

$m, m \in S_i^M$: Index of lane groups at link i,

$\delta_m^{ij}, j \in \Gamma^{-1}(i)$: A binary value indicating whether the movement from link i to j uses lane group m,

N_m^i: Storage capacity of lane group m of link i,

Q_m^i: Discharge capacity of lane group m at link i,

$\Omega^i[k]$: Blocking matrix between lane groups at link i,

$\omega_{m'm}^i[k] \in \Omega^i[k]$: Blocking coefficient between lane group m' and m at step k,

$d_r[k], r \in S_r$: Demand generated at origin r at step k,

$q_r[k], r \in S_r$: Flows enter the link from origin r at step k,

$w_r[k], r \in S_r$: Queue waiting on the origin r at step k,

$q_i^{in}[k]$: Upstream inflows of link i at step k,

$\gamma_{ij}[k], j \in \Gamma^{-1}(i)$: Relative turning proportion of movement from link i to j,

$N_i[k]$: Num. of vehicles at link i for at step k,

$v_i[k]$: Mean approaching speed of vehicles from upstream to the end of queue at link i at step k,

$\rho_i[k]$: Density of the segment from upstream to the end of queue at link i at step k,

$q_i^{arr}[k]$: Traffic arriving at end of queue of link i at step k,

$s_i[k]$: Available space of link i at step k,

$x_i[k]$: Total num. of vehicles in queue at link i at step k,

$q_m^i[k]$: Flows join the queue of lane group m of link i at step k,

$x_m^i[k]$: Queue length of lane group m at link i at step k,

$\tilde{x}_m^i[k]$: Num. of arrival vehicles with destination to lane group m queued outside the approach lanes due to blockage at link i at step k,

$\lambda_m^{ij}[k], j \in \Gamma^{-1}(i)$: Percentage of movement from link i to j in lane group m,

$Q_m^i[k]$: Flows depart from lane group m at link i at step k,

$Q_{ij}^{pot}[k]$: Flows potentially depart from link i to link j at step k,

$Q_{ij}[k]$: Flows actually depart from link i to link j at step k,

$g_m^p[k]$: Binary value indicating whether lane group m at signal phase p is set to green at step k.

In the proposed model, the process of traffic flow propagating along the arterial link is described by six sets of formulations: demand origins, upstream arrivals, propagation to the end of queue, merging into lane groups, departing from a link, and flow conservation. (see Fig. 1)

B. *Demand Origins*

Local demand origins are modeled as follows:

$$q_r[k] = \min\left[d_r[k] + \frac{w_r[k]}{\Delta t}, Q_i, \frac{s_i[k]}{\Delta t} \right] \quad 1)$$

$$w_r[k+1] = w_r[k] + \Delta t[d_r[k] - q_r[k]] \quad 2)$$

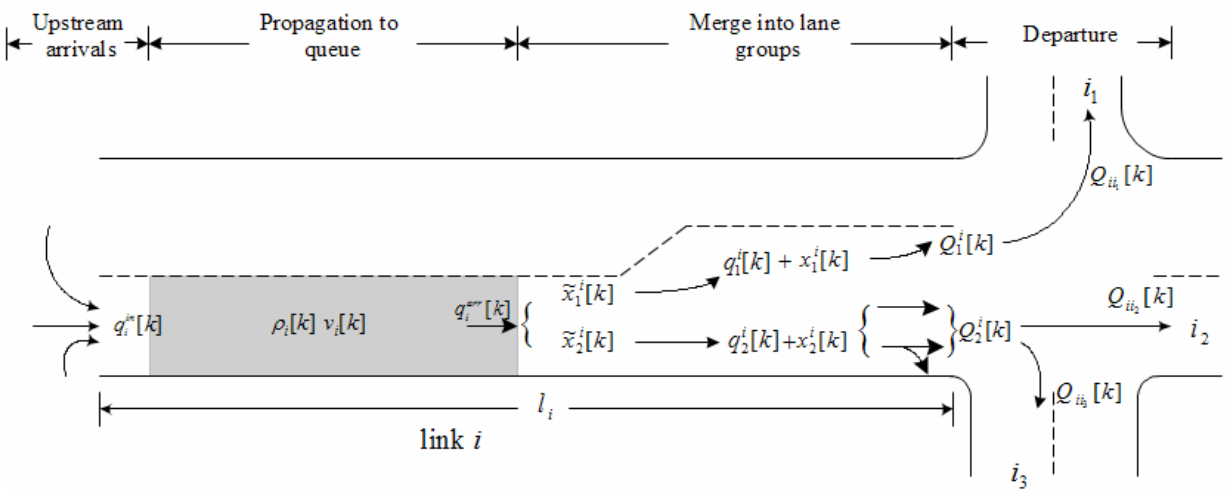

Fig. 1. Traffic flow dynamics along an arterial link

A. Upstream Arrivals

Upstream arrival equations depict the evolution of arriving flows to the upstream of the link over time. Equations (3) to (4) define the flow dynamics for different types of links.

For internal links (with both sets of upstream and downstream links),

$$q_i^{in}[k] = \sum_{j \in \Gamma(i)} Q_{ji}[k] \quad 3)$$

For source links (connected with demand origin r),

$$q_i^{in}[k] = q_r[k] \cdot \Delta t \quad 4)$$

B. Propagation to the End of Queue

This set of dynamic equations represents the evolution of upstream inflows to the end of queue with the average approaching speed over time. The mean speed of vehicles $v_i[k]$ depends on the density of the segment between the link upstream and the end of queue, described by the following equation [7]:

$$v_i[k] = v^{\min} + (v_i^{free} - v^{\min}) \cdot \left[1 - \left(\frac{\rho_i[k]}{\rho^{jam}}\right)^{\alpha}\right]^{\beta} \quad 5)$$

The density of the segment from link upstream to the end of queue is calculated by the following equation:

$$\rho_i[k] = \frac{N_i[k] - x_i[k]}{n_i l_i - \frac{x_i[k]}{\rho^{jam}}} \quad 6)$$

Then, the number of vehicles arriving at the end of queue at link i can be dynamically updated with:

$$q_i^{arr}[k] = \begin{cases} \min\{\rho_i[k] \cdot v_i[k] \cdot n_i \cdot \Delta t, N_i[k] - x_i[k]\} \\ \qquad if \quad k \geq \left\lceil \frac{l_i}{\Delta t \cdot v_i^{free}} \right\rceil \\ 0 \qquad o.w. \end{cases} \quad 7)$$

Where, $\left\lceil \frac{l_i}{\Delta t \cdot v_i^{free}} \right\rceil$ denotes the number of time steps to travel from upstream of link to the stop-line at the free flow speed. Here, we set $q_i^{arr}[k] = 0$ when $k < \left\lceil \frac{l_i}{\Delta t \cdot v_i^{free}} \right\rceil$ in order to avoid over-estimation of arrival flows to the end of queue during the initialization period.

C. Merging into Lane Groups

After vehicles arrive at the end of queue at a link, they will try to change lanes and merge into different lane groups according to their destinations. Most previous studies assume that the arrival vehicles could always merge into their destination lanes without being blocked. However, this assumption could be violated in two ways: (a) overflow: the lane group is full and has no more space to accommodate vehicles (e.g. a fully occupied left-turn bay); (b) blockage: the overflowed queues from other lane groups are blocking the entrance to this lane group even though spaces are available in it (as shown in Fig. 2). Therefore, arrival vehicles that could not merge into their destination lane group m due to either overflows or blockage will form queues outside the approach lanes, denoted by $\tilde{x}_m^i[k]$.

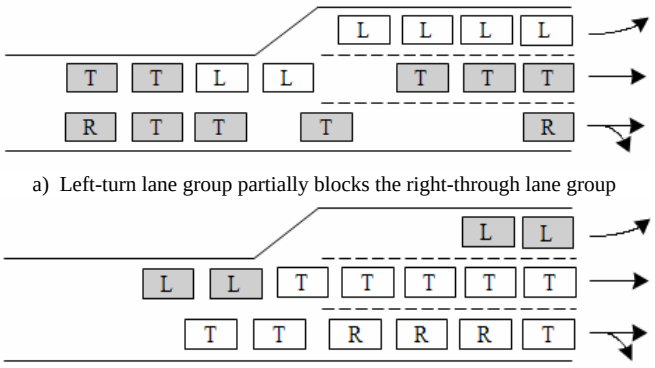

a) Left-turn lane group partially blocks the right-through lane group

b) Right-through lane group completely blocks the left-turn lane group

Fig. 2. Blockage between lane groups

Firstly, the number of vehicles allowed to merge into lane group m at time step k depends on the available storage capacity of the lane group, given by:

$$\max\{N_m^i - x_m^i[k], 0\} \quad 8)$$

Secondly, to reflect the aforementioned blocking effect between different lane groups, we classify it into two types: complete blockage and partial blockage (see Fig. 2). A concept of blocking matrix was introduced here, denoted by $\Omega^i[k]$. The matrix element $\omega^i_{m'm}[k]$ which takes a value between 0 and 1 depicts the blocking impact of lane group m' on lane group m at time step k. In this paper, we modeled $\omega^i_{m'm}[k]$ as follows:

$$\omega^i_{m'm}[k]=\begin{cases}1 & complete\ \ blockage\\ \phi_{m'm}\cdot\dfrac{\tilde{x}^i_{m'}[k]}{\sum_{m\in S_i^M}\tilde{x}^i_m[k]} & partial\ \ blockage\\ 0 & no\ \ blockage\ \ \ or\ \ \ x^i_{m'}[k]\le N^i_{m'}\end{cases} \quad 9)$$

At each time step, the macroscopic model will evaluate all the elements in the blocking matrix. For the complete blockage or no blockage cases, $\omega^j_{m'm}[k]$ can be easily determined to 1 or 0 based on the geometric features of the approach (see Fig. 2b). However, for the partial blockage case, $\omega^j_{m'm}[k]$ will be updated dynamically depending on how overflowed vehicles are distributed out of the approach lanes. Here, we assume that queuing vehicles outside the approach lanes due to overflow or blockage will occupy the link uniformly. Therefore, $\tilde{x}^i_{m'}[k]/\sum_{m\in S_i^M}\tilde{x}^i_m[k]$ depicts the percentage of lanes being blocked by the overflowed lane group m' at time step k. $\phi_{m'm}$ is a constant parameter between 0 and 1 that is related to driver's response to lane blockage and geometry features (to be calibrated).

We take the link shown in Fig. 2 as an example, there are two lane groups in the link: left-turn and right-through (named as *L* and *R-T*, respectively). Therefore, the blocking matrix at time step k is constructed as $\begin{bmatrix}/ & \omega^i_{L,R-T}[k]\\ \omega^i_{R-T,L}[k] & /\end{bmatrix}$

Where,

$$\omega^i_{L,R-T}[k]=\begin{cases}\phi_{L,R-T}\cdot\dfrac{\tilde{x}^i_L[k]}{\tilde{x}^i_L[k]+\tilde{x}^i_{R-T}[k]}, & if\ \ x^i_L[k]>N^i_L\\ 0 & if\ \ x^i_L[k]\le N^i_L\end{cases}$$

$$\omega^i_{R-T,L}[k]=\begin{cases}1 & if\ \ x^i_{R-T}[k]>N^i_{R-T}\\ 0 & if\ \ x^i_{R-T}[k]\le N^i_{R-T}\end{cases}$$

Considering the impact of blocking matrix, the number of vehicles allowed to merge into lane group m at time step k is restricted by:

$$\left[\tilde{x}^i_m[k]+\sum_{j\in\Gamma^{-1}(i)}q^{arr}_i[k]\cdot\gamma_{ij}[k]\cdot\delta^{ij}_m\right]\cdot\left[1-\sum_{m'\in S_i^M\wedge m'\ne m}\omega^i_{m'm}[k]\right] \quad 10)$$

Where, $[\tilde{x}^i_m[k]+\sum_{j\in\Gamma^{-1}(i)}q^{arr}_i[k]\cdot\gamma_{ij}[k]\cdot\delta^{ij}_m]$ is the number of vehicles potentially to merge into lane group m at time step k, and $1-\sum_{m'\in S_i^M\wedge m'\ne m}\omega^i_{m'm}[k]$ is the residual fraction of lanes open to accommodate the merging vehicles.

Finally, the number of vehicles allowed to merge into lane group m at time step k is determined to be the minimum value of Eq. 8) and Eq.10) , given by:

$$q^i_m[k]=\min\left\{\begin{bmatrix}\max\{N^i_m-x^i_m[k],0\}\\ \tilde{x}^i_m[k]+\sum_{j\in\Gamma^{-1}(i)}q^{arr}_i[k]\cdot\gamma_{ij}[k]\cdot\delta^{ij}_m\end{bmatrix}\cdot\left[1-\sum_{m'\in S_i^M\wedge m'\ne m}\omega^i_{m'm}[k]\right]\right. \quad 11)$$

D. Departing from Links

The number of vehicles potentially departing from link i to link j at time step k is given by:

$$Q^{pot}_{ij}[k]=\sum_{m\in S_i^M}\min\left\{q^i_m[k]+x^i_m[k],Q^i_m\cdot g^p_m[k]\right\}\cdot\lambda^{ij}_m[k] \quad 12)$$

$$\lambda^{ij}_m[k]=\frac{\delta^{ij}_m\cdot\gamma_{ij}[k]}{\sum_{j\in\Gamma^{-1}(i)}\delta^{ij}_m\cdot\gamma_{ij}[k]} \quad 13)$$

However, the actual number of vehicles departing from link i to link j at time step k is constrained by the available storage space of the destination link j. Since the total flow towards one destination link j may consist of several flows from different upstream links, this study assumes that the free storage space of link j allocated to accommodate upstream departing flow from link i is proportional to its potential departing flow. Therefore, the actual departing flows from link i to link j at time step k is given by the following equation:

$$Q_{ij}[k]=\max\left\{0,\min\left\{Q^{pot}_{ij}[k],\frac{Q^{pot}_{ij}[k]}{\sum_{i\in\Gamma(j)}Q^{pot}_{ij}[k]}\cdot s_j[k]\right\}\right\} \quad 14)$$

Then, the actual departing flow from lane group m at link i can be easily obtained by:

$$Q^i_m[k]=\sum_{j\in\Gamma^{-1}(i)}Q_{ij}[k]\cdot\delta^{ij}_m \quad 15)$$

E. Flow Conservation

For the approach lanes, the lane group based queues are advanced as follows:

$$x^i_m[k+1]=x^i_m[k]+q^i_m[k]-Q^i_m[k] \quad 16)$$

Queues outside the approach lanes are advanced as follows:

$$\tilde{x}^i_m[k+1]=\tilde{x}^i_m[k]-q^i_m[k]+\sum_{j\in\Gamma^{-1}(i)}q^{arr}_i[k]\cdot\gamma_{ij}[k]\cdot\delta^{ij}_m \quad 17)$$

Then, the total number vehicles queued at link i is computed as:

$$x_i[k+1]=\sum_{m\in S_i^M}\left[x^i_m[k+1]+\tilde{x}^i_m[k+1]\right] \quad 18)$$

The total number of vehicles present at link i is advanced

as follows:

$$N_i[k+1] = N_i[k] + \sum_{j\in\Gamma(i)} Q_{ji}[k] - \sum_{j\in\Gamma^{-1}(i)} Q_{ij}[k] \quad 19)$$

And, the available storage space of link i is computed as:

$$s_i[k+1] = N_i - N_i[k+1] \quad 20)$$

III. MODEL VALIDATION

A. Test Intersection

In this section, performance of proposed macroscopic model is evaluated at a real-world intersection (MD212 and Adelphi Rd., Maryland) under different demand scenarios on a microscopic simulator VISSIM. Fig. 3 shows the geometric configuration and lane chanellization of test intersection, and Table I lists the signal timings of the target intersection. The reason for choosing this intersection as a test site is that both shared lanes and left-turn bays exist in this intersection. Also, severe blockages occur between the left-turn and right-through traffic at eastbound and westbound approaches during the congested hours.

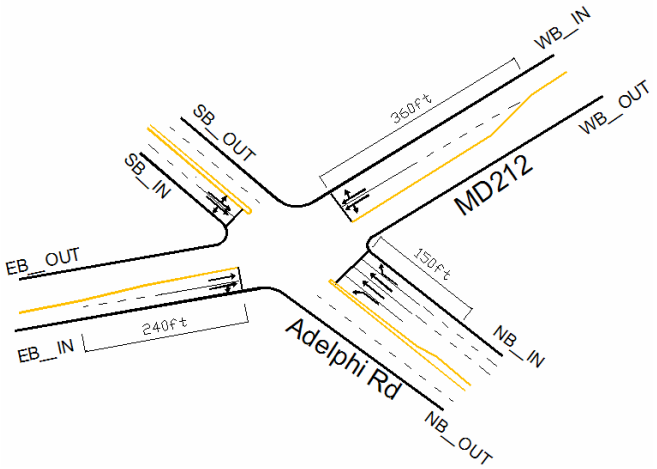

Fig. 3. Test Intersection for Model Validation (MD212@Adelphi Rd.)

TABLE I
SIGNAL SETTINGS FOR THE TEST INTERSECTION

Phases	I	II	III
Green Time (secs)	44	35	49
Yellow Time (secs)	3	3	3
All-red Time (secs)	1	1	1
Movements			

B. Simulation Calibration and Model Parameter Fitting

To make sure VISSIM reliably replicate driver behavioral patterns and traffic conditions at the test intersection, we calibrate it using data collected at the intersection during a two-hour period in the morning (7:30 am to 9:30 am). Due to the limitation of data availability, traffic data used for calibrating the target simulated intersection are only traffic volumes at a time interval of 5 minutes, which are collected for all movements at each approach. To make the results of VISSIM comparable to the outputs from the proposed deterministic macroscopic model, we set the vehicle entry headway distribution as uniform for each time interval.

For calibration of the proposed macrosopic model, the parameters vector for link *i* is shown as follows:

$$\theta_i = [Q_i, \rho_i^{jam}, v_i^{free}, v_i^{\min}, \alpha, \beta, Q_i^m, \Omega^i] \quad 21)$$

Let $[Q_{ij}[t]]$ denote the model-output values of departure volumes for movement from link *i* to *j*, and $[\overline{Q}_{ij}[t]]$ represent the field measured values then θ_i is chosen for each link *i* to minimize the quadratic errors between the model-output and the field collected values of traffic volumes for all movements of that intersection:

$$L(\theta) = \frac{1}{n^U n^T} \sum_{i\in S^U} \sum_{t=1}^{n^T} (Q_{ij}[t] - \overline{Q}_{ij}[t])^2 \quad 22)$$

Where, n^U is the number of links and $t = 1,\ldots,n^T$ is the sampling intervals (5 minutes in this study). To avoid the local optimal or abnormal values from the non-linear optimization problem for parameter fitting, some parameters can be pre-fixed or bounded by commonly used equations or practices. For example, the discharge capacity for lane group m can be easily bounded around the values calculated from the Highway Capacity Manual (HCM).

Table II summarize the model parameter values after calibration:

TABLE II
PARAMETER FITTING RESULTS FOR ALL LINKS

Links	Q_i (veh/hr)	ρ^{jam} (veh/mile/lane)	$v^{\min}$ (mph)	v_i^{free} (mph)	α	β	$[Q_i^m]$ (veh/hr)	Ω^i (blocking matrix)
EB_IN	1873			35			$\begin{bmatrix} L & R-T \\ 647 & 1805 \end{bmatrix}$	$\begin{matrix} & L & R\text{-}T \\ L & / & 1.0 \\ R\text{-}T & 1.0 & / \end{matrix}$
EB_OUT	1881			35			1881	Not applicable
WB_IN	1857			35			$\begin{bmatrix} L & R-T \\ 935 & 1844 \end{bmatrix}$	$\begin{matrix} & L & R\text{-}T \\ L & / & 1.0 \\ R\text{-}T & 1.0 & / \end{matrix}$
WB_OUT	1870			35			1870	Not applicable
NB_IN	5105	225	5	30	1.2	1.8	$\begin{bmatrix} L & T & R \\ 533 & 3540 & 1581 \end{bmatrix}$	$\begin{matrix} & L & T & R \\ L & / & 0.18\frac{\bar{v}_T[k]}{\sum_{m\in T}\bar{v}_m[k]} & 0 \\ T & 1.0 & / & 0 \\ R & 0 & 0 & / \end{matrix}$
NB_OUT	3580			30			3580	Not applicable
SB_IN	3556			30			$\begin{bmatrix} L-T-R \\ 2520 \end{bmatrix}$	Not applicable
SB_OUT	3580			30			3580	Not applicable

C. Experiment Design

After the limited calibration process for the VISSIM model and the proposed macroscopic model, four scenarios with incrementally 10% increasing volumes (denoted by I, II, III, and IV) and two scenarios with incrementally 10% decreasing volumes (denoted by V and VI) from the current intersection demand level are designed to test the proposed model under congested and light traffic conditions. Simulation outputs from VISSIM are deemed to be able to

replicate the field conditions for all those scenarios and were compared with the output values from the proposed model for each scenario.

D. Validation Results and Discussion

Fig. 4 below shows the comparison of 5-minute departure flows for all movements from VISSIM results and the proposed model under each designed scenario. From correlation coefficients shown in the figure, it could be seen that there exist consistency between the results from the VISSIM and the proposed model for all test scenarios. The Root Mean Square Errors (RMSE) and maximal errors are summarized in Table III to provide quantitative evaluation of the proposed model.

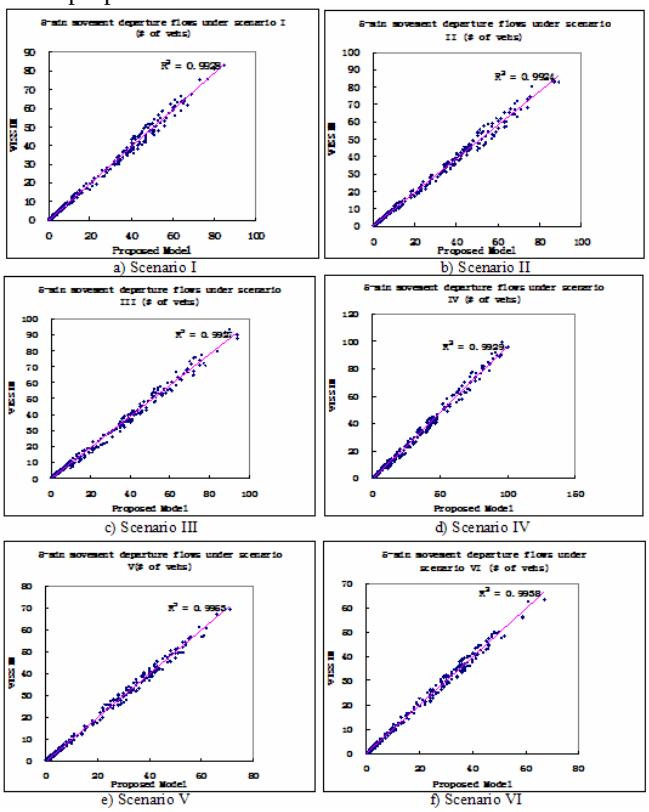

Fig. 4. Comparison of 5-minute movement departure flows from VISSIM and the proposed model

From Table III, it can be observed that RMSE of 5-min movement departure flows are all below 3 vehs, and maximal errors are all within 5 vehs, especially for the eastbound and westbound approaches which have severe blockages during the congested scenarios. The model also provides acceptable accuracy in handing shared lanes in the southbound approach using the lane-group concept. These results show evidence of the promising property of the proposed model and particularly its capability to deal with lane blocking effects and shared lanes.

TABLE III
COMPARISON OF 5-MIN MOVEMENT DEPARTURE FLOW FROM VISSIM AND THE PROPOSED MODEL (UNIT: # OF VEHS)

Movements	Results	Scenarios					
		I	II	III	IV	V	VI
Northbound Left	RMSE	0.57	0.72	1.54	1.42	0.56	0.60
	Max. Error	1	2	3	3	1	1
Northbound Through	RMSE	1.56	2.41	2.42	2.37	2.06	1.93
	Max. Error	3	4	4	4	3	3
Northbound Right	RMSE	0.58	0.70	0.69	1.13	0.61	0.59
	Max. Error	1	2	2	2	1	1
Southbound Left	RMSE	1.17	1.14	1.70	1.81	0.96	0.86
	Max. Error	2	2	3	3	2	2
Southbound Through	RMSE	2.36	2.15	2.71	2.53	1.96	2.04
	Max. Error	4	4	5	5	3	3
Southbound Right	RMSE	0.63	0.61	0.67	0.97	0.51	0.58
	Max. Error	1	1	1	2	1	1
Eastbound Left	RMSE	2.20	1.94	2.63	2.79	1.46	1.35
	Max. Error	3	3	4	5	3	3
Eastbound Through	RMSE	1.78	1.70	2.32	2.67	1.40	1.34
	Max. Error	3	3	4	5	3	3
Eastbound Right	RMSE	0.81	0.75	0.76	0.76	0.69	0.50
	Max. Error	2	2	2	2	1	1
Westbound Left	RMSE	2.15	2.07	2.60	2.67	1.46	1.50
	Max. Error	3	3	4	5	3	3
Westbound Through	RMSE	2.21	2.08	2.25	2.13	1.35	1.24
	Max. Error	3	3	4	4	3	3
Westbound Right	RMSE	0.55	0.65	0.56	0.58	0.62	0.63
	Max. Error	1	1	1	1	1	1
OVERALL	RMSE	1.55	1.56	2.03	2.08	1.25	1.22
	Max. Error	4	4	5	5	3	3

IV. CONCLUSION

In this paper, a macroscopic model which can deal with shared lanes and blocking effects between different lane groups at signalized intersections is developed. The performance of the proposed model applied to a real-world intersection under different demand levels appears to be promising when validated by a calibrated microscopic simulation program, VISSIM. A future research could be integrating the proposed model with optimal control models for traffic signal optimization or applying it to large-scale urban network simulations, as it offers potentials for macroscopic analysis of signalized intersections with computer-efficiency and better accuracy.

REFERENCES

[1] H.R. Kashani and G.N. Saridis. “Intelligent control for urban traffic systems,” *Automatica*, vol. 19, no. 2, pp. 191-197, Mar. 1983.

[2] C. Daganzo, “The Cell Transmission Model: a dynamic representation of highway traffic consistent with hydrodynamic theory,” *Trans. Res. B*, vol. 28-4, pp. 269-287, 1994.

[3] H. Lo, E. Chang, and Y. Chan, “Dynamic network traffic control,” *Trans. Res. A*, vol. 35, pp. 721-744, 2001.

[4] J. Wu and G. L. Chang, “An integrated optimal control and algorithm for commuting corridors,” *Int. Trans. On Oper. Res.*, vol. 6, pp. 39-55, 1999.

[5] Van den Berg, A. Hegyi, B. De Schutter, and J. Hellendoorn, “A macroscopic traffic flow model for integrated control of freeway and urban traffic networks,” in *Proc. IEEE 42nd Int. Conf. on Decision and Control*, Hawaii, pp. 2774-2779, Dec. 2003.

[6] Burghout, W. “Hybrid Microscopic-mesoscopic Traffic Simulation”. Ph. D. Dissertation, Royal Institute of Technology, Stockbolm, Sweden, 2004.

[7] Q. Yang, “A Simulation Laboratory for Evaluation of Dynamic Traffic Management Systems”, Ph. D. Dissertation, Massachusetts Institute of Technology, 1997.